Interior and Interfacial Aqueous Solvation of Benzene Dicarboxylate Dianions and Their Methylated Analogues: A Combined Molecular Dynamics and Photoelectron Spectroscopy Study

Babak Minofar, Luboš Vrbka, Martin Mucha, and Pavel Jungwirth*

Institute of Organic Chemistry and Biochemistry, Academy of Sciences of the Czech Republic and Center for Biomolecules and Complex Molecular Systems, Flemingovo nám. 2, 16610 Prague 6, Czech Republic

Xin Yang, Xue-Bin Wang, You-Jun Fu, and Lai-Sheng Wang*

Department of Physics, Washington State University, 2710 University Drive, Richland, Washington 99352, and W. R. Wiley Environmental Molecular Sciences Laboratory, Pacific Northwest National Laboratory, MS K8-88, P.O. Box, Richland, Washington 99352

Received: February 17, 2005; In Final Form: April 15, 2005

Aqueous solvation of benzene dicarboxylate dianions (BCD^{2-}) was studied by means of photoelectron spectroscopy and molecular dynamics simulations. Photoelectron spectra of hydrated *o*- and *p*-BCD^{2-} with up to 25 water molecules were obtained. An even−odd effect was observed for the *p*-BCD^{2-} system as a result of the alternate solvation of the two negative charges. However, the high polarizability of the benzene ring makes the two carboxylate groups interact with each other in *p*-BCD^{2-}, suppressing the strength of this even−odd effect compared with the linear dicarboxylate dianions linked by an aliphatic chain. No even−odd effect was observed for the *o*-BCD^{2-} system, because each solvent molecule can interact with the two carboxylate groups at the same time due to their proximity. For large solvated clusters, the spectral features of the solute decreased while the solvent features became dominant, suggesting that both *o*- and *p*-BCD^{2-} are situated in the center of the solvated clusters. Molecular dynamics simulations with both nonpolarizable and polarizable force fields confirmed that all three isomers (*o*-, *m*-, and *p*-BCD^{2-}) solvate in the aqueous bulk. However, upon methylation the hydrophobic forces overwhelm electrostatic interactions and, as a result, the calculations predict that the tetramethyl-*o*-BCD^{2-} is located at the water surface with the carboxylate groups anchored in the liquid and the methylated benzene ring tilted away from the aqueous phase.

Introduction

The carboxylate functional group ($-COO^-$) is ubiquitous in biological systems, as well as in many technologically important materials, and in polluted atmospheres. An interesting group of systems is formed by species containing more than one carboxylate group. In particular, dicarboxylic acids have been recognized as a class of global atmospheric pollutants, and they are among the major organic compounds in urban aerosol samples.[1,2] Dicarboxylic acids are produced from photochemical reactions and from pyrolysis of plants and other organic materials. For example, low molecular weight dicarboxylic acids, such as glutaric acid, form by photooxidation of cyclohexene and cyclopentene.[3] Due to the presence of two carboxylate groups, dicaboxylic acids are less volatile than the corresponding monocarboxylic acids. In the atmosphere, they are primarily found in aerosols[4] unlike, e.g., the formic and acetic acids, which are mostly present in the gaseous phase. Dicarboxylic acids in atmospheric particles play an important role as cloud condensation nuclei.[5,6] Furthermore, they are responsible for the formation of many secondary organic aerosols.[7] Thus understanding the microsolvation of dicarboxylic acids and their behavior at the water/vapor interface is very important for atmospheric chemistry.

Previously, we have investigated by means of photoelectron spectroscopy, molecular dynamics, and electronic structure calculations dicarboxylate dianions in which the two COO^- groups are connected by an aliphatic chain of varying lengths (oxalate, succinate, adipate, suberate, etc.).[8,9] The focus was on the sequential solvation of these dianions in size-selected water clusters and on bulk vs interfacial solvation in extended aqueous systems. The flexible aliphatic chains give rise to an interesting phenomenon of solvent-induced conformation changes for large solvated clusters as a result of the competition between Coulomb repulsion, water−water H-bonding and hydrophobic and hydrophilic solvation. In this study, we investigate dicarboxylate dianions in which the spacer between the two carboxylate groups is a rigid aromatic ring. The generic system is the *o*-benzene dicarboxylate dianion. This is the doubly ionized form of the technologically and environmentally extremely important phthalic acid, the esters of which used as a polyvinyl chloride (PVC) softener represent a widely discussed potential health hazard.[10,11] Here, we study the aqueous solvation of all three *o*-, *m*-, and *p*-benzene dicarboxylate dianions (*o*-, *m*-, and *p*-BCD^{2-}) and of the tetramethylated *o*-BCD^{2-}. Using photoelectron spectroscopy and ab initio calculations, we investigate solvation of benzene dicarboxylate dianions in water clusters and the role of the aromatic ring in electronically connecting the partially hydrated carboxylate groups. By means of molecular dynamics simulations we explore the competition between

* To whom correspondence should be addressed. E-mails: (P.J.) pavel.jungwirth@uochb.cas.cz; (L.-S.W.) ls.wang@pnl.gov.

10.1021/jp050836u CCC: $30.25
Published on Web 05/20/2005

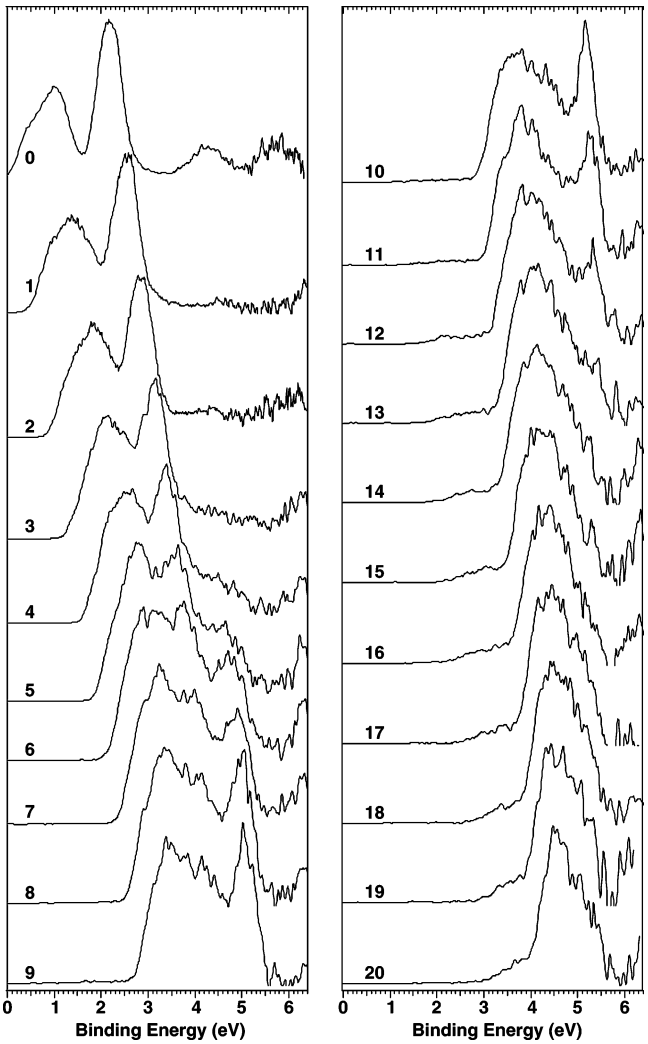

Figure 1. Photoelectron spectra of *o*-$BCD^{2-}(H_2O)_x$ ($x = 0-20$) at 193 nm (6.424 eV).

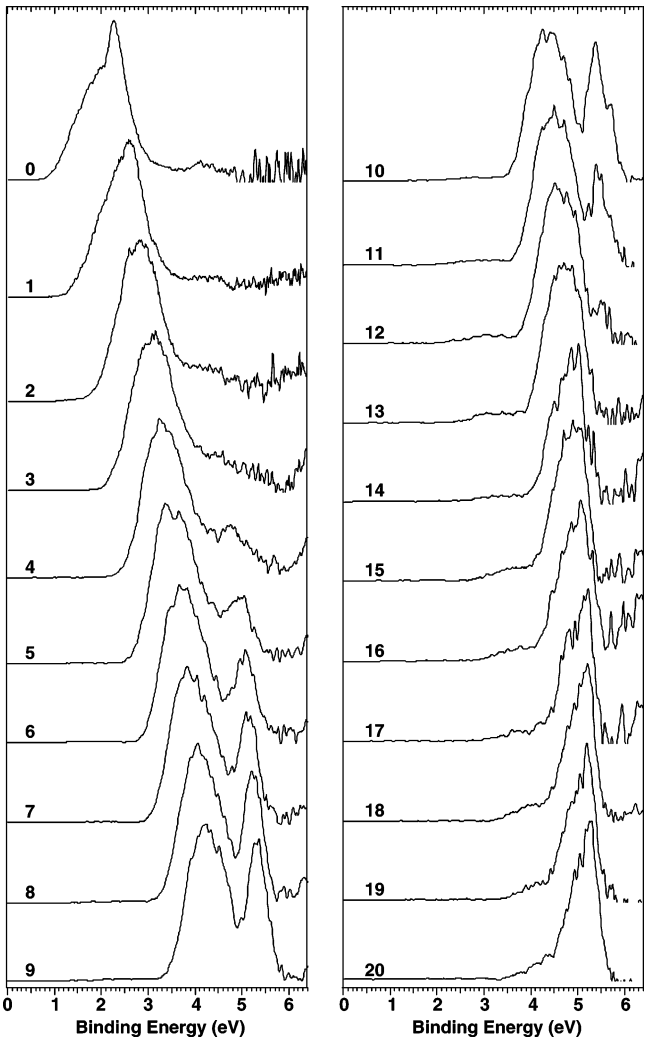

Figure 2. Photoelectron spectra of *p*-$BCD^{2-}(H_2O)_x$ ($x = 0-20$) at 193 nm (6.424 eV).

electrostatic and hydrophobic interactions in bulk versus interfacial solvation of the parent and methylated dianions in aqueous slabs.

Experimental Methods

The experiment was carried out using an apparatus equipped with a magnetic bottle time-of-flight photoelectron analyzer and an electrospray ionization (ESI) source.[12] Details of the experimental method have been given elsewhere,[12] and the procedures were similar to our previous studies on the solvated dicarboxylate dianions.[8,9] We chose two of the three benzene dicarboxylate acids, *o*-BCD^{2-} and *p*-BCD^{2-}, for the photoelectron spectroscopy (PES) experiments to represent two extreme cases, in which the two carboxylate groups are the closest and farthest to each other around the benzene ring, respectively. Briefly, solvated dianions with a wide range of solvent numbers, *o*-(*p*-)$BCD^{2-}(H_2O)_x$, were produced from electrospray of mixed solutions of 10^{-3} M of the corresponding disodium salts in a water−acetonitrile mixed solvent (1:4 volume ratio). Anions produced from the ESI source were guided into a room-temperature ion trap, where ions were accumulated for 0.1 s before being pulsed into the extraction zone of a time-of-flight mass spectrometer. During photoelectron spectroscopic experiments, the dianions of interest were mass-selected and decelerated before being intercepted by a probe laser beam in the photodetachment zone of the magnetic bottle photoelectron analyzer. In the current study, the detachment photon energies used were 193 nm (6.424 eV) and 157 nm (7.867 eV). Photoelectron time-of-flight spectra were collected and then converted to kinetic energy spectra, calibrated by the known spectra of I^- and O^-. The electron binding energies (EB) were obtained by subtracting the kinetic energy (KE) spectra from the detachment photon energy ($EB = h\nu - KE$). The energy resolution ($\Delta KE/KE$) was about 2%, i.e., ~10 meV for 0.5 eV electrons, as measured from the spectrum of I^- at 355 nm.

Computational Methods

Classical molecular dynamics simulations were aimed at a Boltzman sampling of solvation structures of the *o*-, *m*-, and *p*-benzene dicarboxylate dianions, as well as the tetramethyl-*o*-benzene dicarboxylate dianion in aqueous slabs. To construct the slab a (tetragonal) prismatic box of $30 \times 30 \times 120$ Å^3 was used, containing 863 water molecules, two identical dianions (placed initially on each side of the slab), and four sodium counterions. Application of periodic boundary conditions at a constant volume with such a unit cell yields an infinite slab with two water/vapor interfaces perpendicular to the *z* axis.[13] The nonbonded interactions were cut off at 12 Å, and long-range electrostatic interactions were accounted for using the particle mesh Ewald procedure.[14] All systems were first minimized (10,000 steps of steepest descent) in order to avoid bad contacts and equilibrated for several hundreds of picosec-

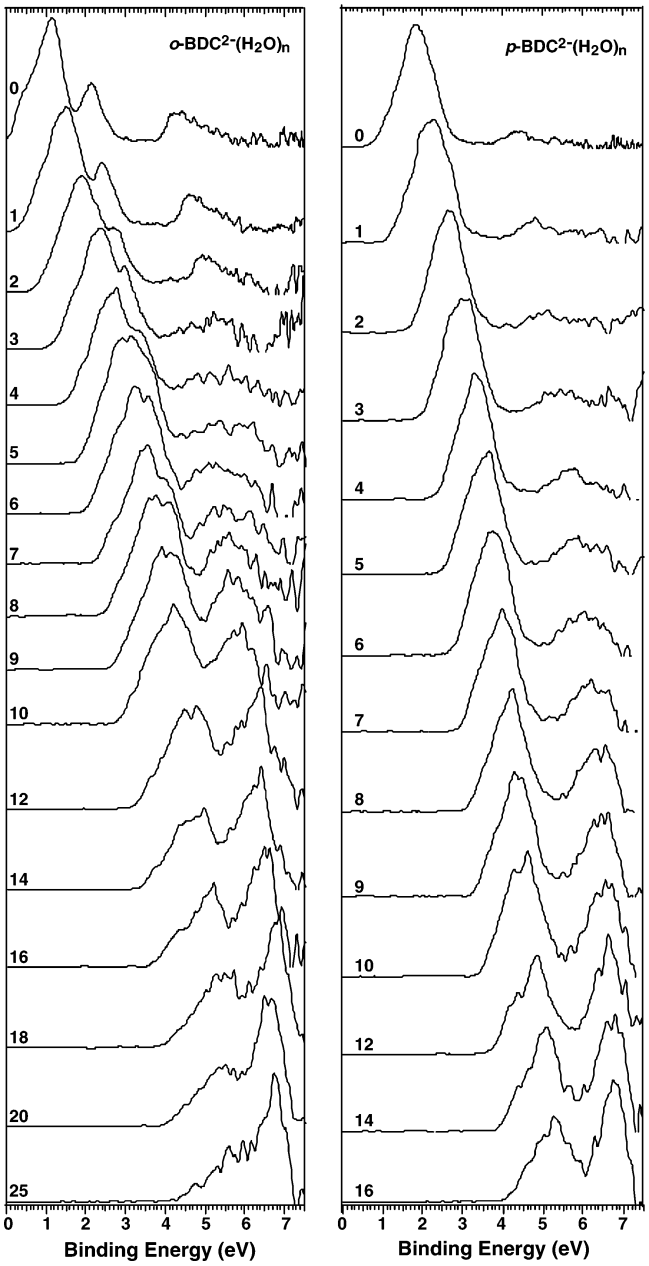

Figure 3. Photoelectron spectra of selected *o*-$BCD^{2-}(H_2O)_x$ (x = 0−25) and *p*-$BCD^{2-}(H_2O)_x$ (x = 0−16) at 157 nm (7.866 eV).

onds before a 1 ns production run. Simulations were performed at 300 K with a time step of 1 fs, and all bonds involving hydrogen atoms were constrained using the SHAKE algorithm.[15]

Both nonpolarizable and polarizable force fields were employed in the MD simulations. For water, we used either the SPCE[16] or the POL3[17] models. For the ions we employed the general amber force field parameter set.[18] Fractional charges for the dianions were evaluated using the standard RESP procedure, and all molecular dynamics calculations were performed using the Amber 8 program,[19] while Gaussian 03 was employed for electronic structure calculations.[20]

Results and Discussion

Photoelectron Spectra at 193 and 157 nm. The photoelectron spectra of *o*-, *p*-$BCD^{2-}(H_2O)_x$ (x = 0−20) at 193 nm are displayed in Figures 1 and 2, respectively. The photoelectron spectra of selected *o*-, *p*-$BCD^{2-}(H_2O)_x$ at 157 nm are displayed in Figure 3.

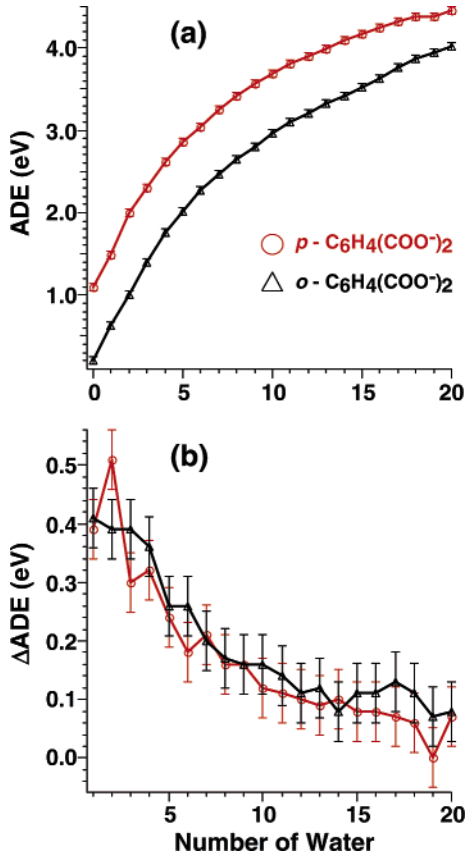

Figure 4. (a) Adiabatic electron binding energies (ADE) of *o*-$BCD^{2-}(H_2O)_x$ (x = 0−20; black) and *p*-$BCD^{2-}(H_2O)_x$ (x = 0−20; red) as a function of solvent numbers (x). (b) Differential ADE [ΔADE = ADE(x) − ADE(x−1)] as a function of x.

The difference of the spectral features and electron binding energies between bare *o*-BCD^{2-} and *p*-BCD^{2-} had been explained in our previous publication.[21] For the spectrum of *o*-BCD^{2-}, the first broad band at very low binding energies is due to detachment of the O lone pairs in the carboxylate groups. The extremely low binding energies are due to the strong Coulomb repulsion between the two carboxylate groups at the ortho position. The band centered at ∼2.2 eV is assigned to be from the π system of the benzene ring. For *p*-BCD^{2-}, the longer distance between the two carboxylate groups reduces the intramolecular Coulomb repulsion and increases the electron binding energies of the O lone pairs. Since the binding energy of the π electron feature does not change in *p*-BCD^{2-} relative to that in *o*-BCD^{2-}, it overlaps with the spectral features from the carboxylate O lone pairs (Figure 2).

Several observations can be made about the spectra of the hydrated species in Figures 1−3. First, the spectral features shift steadily to higher binding energies with increasing solvent molecules in both *o*- and *p*-$BCD^{2-}(H_2O)_x$ due to stabilization of the negative charges by water. Second, spectral features on the high binding energy side are cut off in both 193 and 157 nm spectra as a result of the repulsive Coulomb barrier (RCB), which exists universally in multiply charged anions and essentially prohibits slow electrons from being emitted.[22] The π electron feature quickly disappears with the addition of the first few water molecules due to the cutoff caused by the RCB. For the spectra of larger clusters, only the onset of the carboxylate features can be observed. Third, from x = 5 in *o*-$BCD^{2-}(H_2O)_x$ and x = 4 in *p*-$BCD^{2-}(H_2O)_x$, a new band emerges at the high binding energy side. In the 193 nm spectra (Figures 1 and 2), the relative intensity of the new band reaches maximum at x =

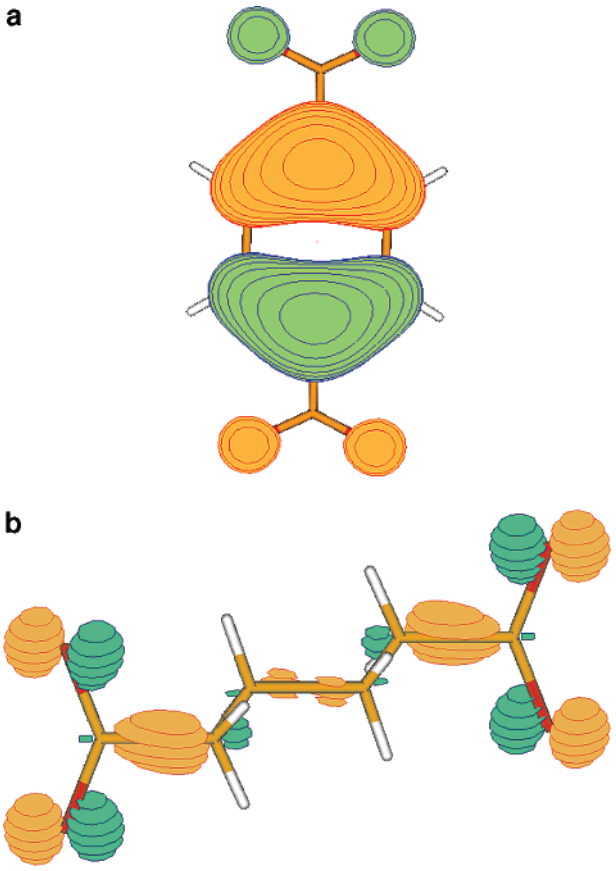

Figure 5. Highest occupied molecular orbital (HOMO) of (a) *p*-BCD^{2-} and (b) the adipate dianion. Note the delocalization of the HOMO of *p*-BCD^{2-} in the aromatic ring and the localized HOMO on the carboxylates in adipate.

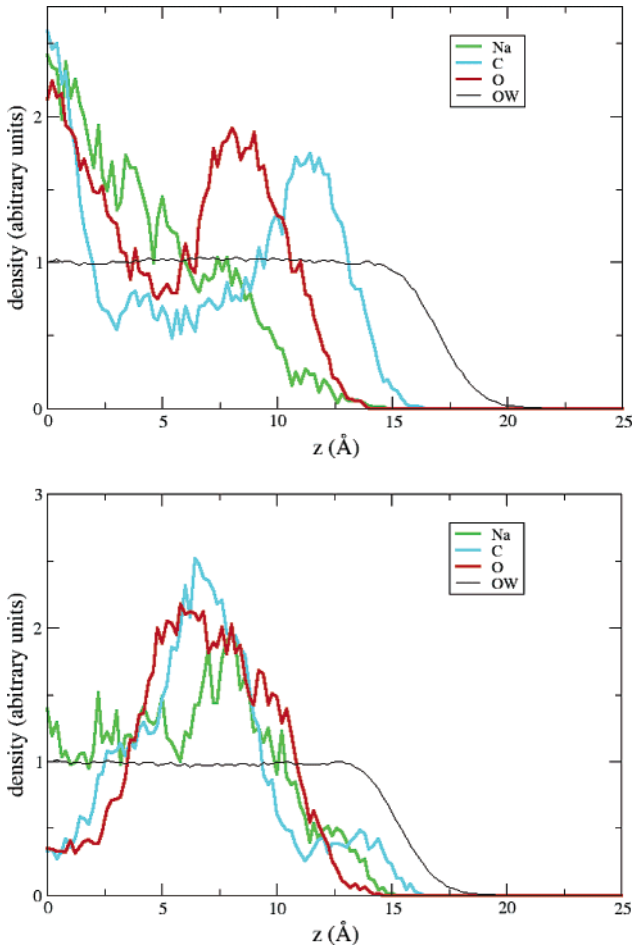

Figure 6. Density profiles (i.e., histogrammed densities of the electrolyte ions and water molecules in layers parallel to the surface, from the center of the slab across the interface into the gas phase) of water oxygens and carbons and oxygens of *o*-BCD^{2-} in an aqueous slab employing (a) polarizable and (b) nonpolarizable force fields.

9 for both systems and gradually disappears with increasing cluster size due to the RCB cutoff. In the 157 nm spectra (Figure 3), the new emerging band becomes the dominant feature for large clusters. Fourth, some weak spectral features appear for large clusters ($x > 10$) in the lower binding energy range in both systems in the 193 nm spectra (Figures 1 and 2), but not showing up in the 157 nm spectra (Figure 3). The photon energy dependence suggests that these features might be due to two-photon processes.

Interactions between the Carboxylate Groups in Solvated Clusters. The adiabatic detachment energies (ADEs), estimated from the threshold of the photoelectron spectra shown in Figures 1 and 2, are plotted as a function of solvent number (x) in Figure 4a. The differential ADE (ΔADE), defined as [ADE(x) − ADE($x-1$)], is the net stabilization of one water to the negative charge as water is sequentially added. It is plotted in Figure 4b as a function of x.

The differential ADE (Figure 4b, red curve) for hydrated *p*-BCD^{2-} shows an even−odd oscillation at small cluster size ($x < 5$). We observed this even−odd effect in a series of solvated linear aliphatic dicarboxylate dianions.[8,9] This is because the two carboxylate groups are solvated separately in these systems, and each water molecule can only solvate one carboxylate. The two carboxylate groups in *p*-BCD^{2-}(H$_2$O)$_x$ should also be solvated alternately by water molecules at small cluster sizes because they are separated by a rigid benzene ring. It is interesting to compare *p*-BCD^{2-}(H$_2$O)$_x$ with solvated adipate dianion [$^-$O$_2$C(CH$_2$)$_4$CO$_2^-$] because the distances between the two carboxylate groups are similar in these two dianions. However, we noted that the even−odd effect shown in the differential ADEs for the adipate systems are much stronger than that shown in the *p*-BCD^{2-}(H$_2$O)$_x$ system.[9] The difference is caused by the different polarizability of the spacer between the two carboxylate groups. On one hand, in adipate the aliphatic chain can be viewed as an insulator. The two carboxylate groups are solvated separately and independently with little electronic communication. On the other hand, in *p*-BCD^{2-} with planar D_{2h} symmetry[21] the two carboxylate groups can interact with each other through the much more polarizable phenyl ring. Once the equivalence between the two carboxylate groups is broken by the solvent molecule for odd solvent numbers, the electron densities can redistribute to compensate the less stabilized charge, which reduces the energy difference between the two carboxylate groups and suppresses the oscillatory pattern in the differential ADEs in *p*-BCD^{2-}(H$_2$O)$_x$. The difference between the aromatic and aliphatic spacer between the two carboxylate groups can also be seen clearly from the corresponding highest occupied molecular orbitals (HOMO). Figure 5 compares the HOMO (evaluated with the 6-31+G* basis set) of *p*-BCD^{2-} with that of the adipate dianion. While for the system with the aromatic spacer the HOMO is delocalized over the carboxylate groups and the benzene ring (Figure 5a), there is virtually no HOMO electron density on the aliphatic chain in adipate (Figure 5b).

The ADEs of the hydrated *o*-BCD^{2-} (Figure 4a, black curve), which are much lower than those for *p*-BCD^{2-}(H$_2$O)$_x$ due to

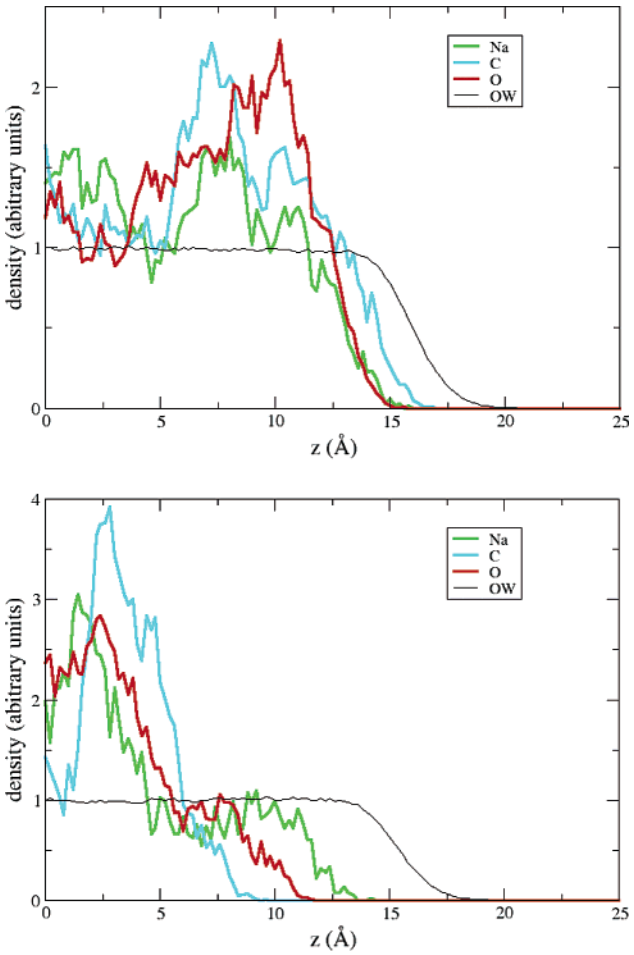

Figure 7. Density profiles of water oxygens and carbons and oxygens of *m*-BCD^{2-} in an aqueous slab employing (a) polarizable and (b) nonpolarizable force fields.

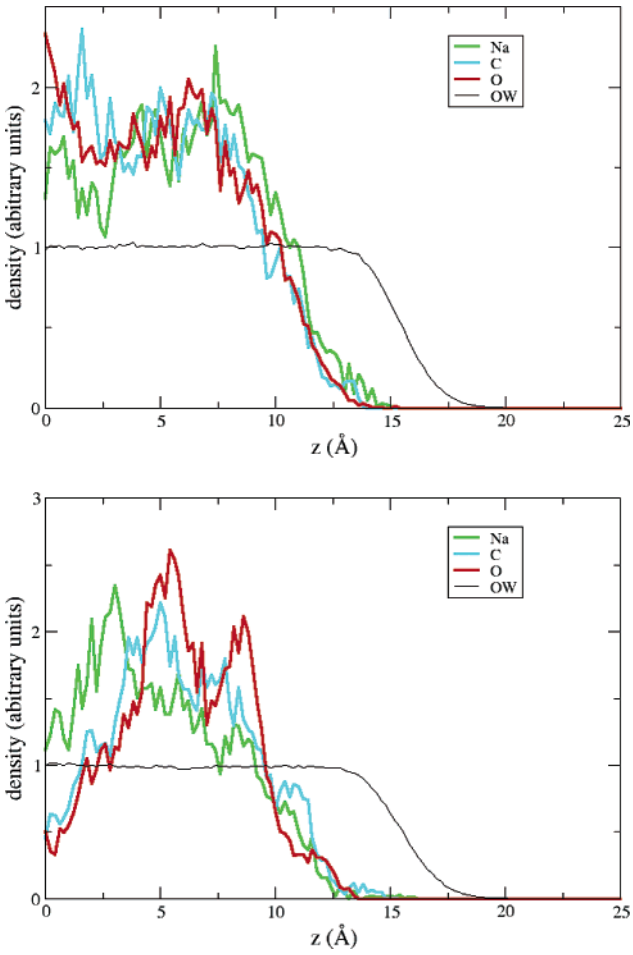

Figure 8. Density profiles of water oxygens and carbons and oxygens of *p*-BCD^{2-} in an aqueous slab employing (a) polarizable and (b) nonpolarizable force fields.

the stronger intramolecular Coulomb repulsion, exhibit a smooth increase with the solvent number. The differential ADE (Figure 4b, black curve) shows a monotonic decrease without any even−odd effect within our experimental uncertainty. According to our previous study, *o*-BCD^{2-} has C_2 symmetry with the carboxylate groups rotated ∼54° away from the plane of the benzene ring due to the strong Coulomb repulsion.[21] Even with this rotated geometry, the two carboxylate groups are close enough that each water molecule can interact with both of them at the same time. Each carboxylate group gains roughly the same stabilization energy with the addition of every solvent molecule. Thus no odd−even effect is expected in these systems.

Interior versus Surface Solvation. The additional features emerging in the spectra of large clusters (Figures 1−3) are similar to those observed in our previous PES studies on different solvated systems. These high binding energy features were found to be due to ionization of solvent water molecules,[23−25] because the ionization potential of water was significantly lowered in the presence of the two negative charges. Beside the rapidly increasing solvent band, another interesting observation is the fact that often the intensity of the solute features decreased gradually with the solvent number.[23−25] We see the same effect in the present systems; e.g., for *o*-BCD^{2-}-$(H_2O)_{25}$ (left column in Figure 3) the solute features become a low binding energy tail in the presence of the dominant solvent band. Previously, we interpreted this phenomenon in hydrated SO_4^{2-} and $C_2O_4^{2-}$ clusters as due to the fact that these solutes are solvated in the center of the solvated clusters.[23−25] The physical picture is as follows: as the solvation shell around the dianion completes, and the ejected photoelectron starts to be strongly scattered by the surrounding water molecules, which leads to the decrease of the solvent feature in the PES. The decrease of the BCD^{2-} photoemission intensity with increasing cluster size thus suggests that both *o*-, *p*-BCD^{2-} are solvated in the center of large water clusters so that the electron signals from the solutes are suppressed by the surrounding solvation layer. Based on this microsolvation information, we can estimate that all the three *o*-, *m*-, *p*-BCD^{2-} species prefer bulk aqueous solvation to that at the water/vapor interface.

Computational Results

The benzene dicarboxylate dianions possess two strongly hydrophilic $-COO^-$ groups connected by a hydrophobic aromatic ring. It is not a priori obvious which of the two interactions with water are stronger and, consequently, whether these dianions prefer bulk or interfacial aqueous solvation, even though the above photoelectron data seem to suggest that in the large solvated clusters they prefer to be in the center of the water clusters. To explore this issue, we performed molecular dynamics simulations of *o*-, *m*-, *p*-BCD^{2-} in aqueous slabs employing both nonpolarizable and polarizable force fields.

Over the nanosecond simulations we averaged the density profiles, i.e., histogrammed abundancies of the individual species in slices parallel with the surface, from the aqueous bulk across the water/vapor interface into the gas phase. The results for *o*-, *m*-, *p*-BCD^{2-} are shown in Figures 6−8. We see that in all cases and with or without explicit polarization the hydrophilicity of

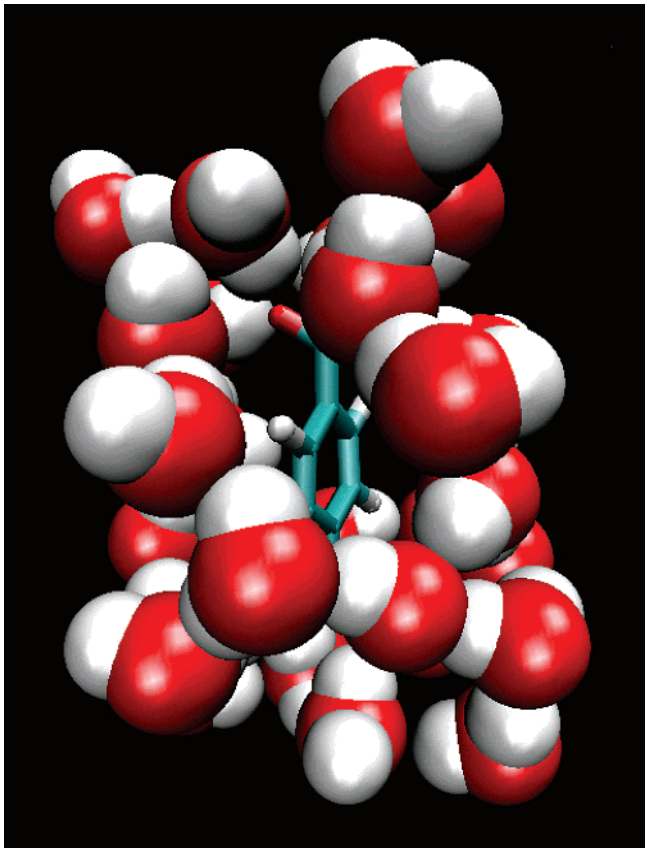

Figure 9. Snapshot of the first solvation shell (25 water molecules) of *p*-BCD^{2-}. Note the reduced water density around the benzene ring compared to that around the $-COO^-$ groups.

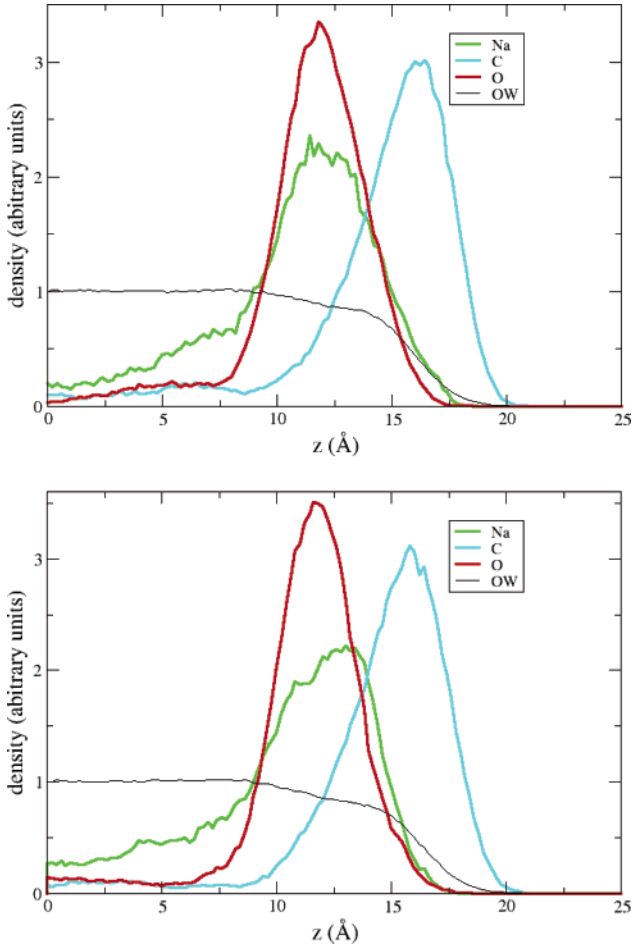

Figure 10. Density profiles of water oxygens and carbons and oxygens of tetramethyl-*o*-BCD^{2-} in an aqueous slab employing (a) polarizable and (b) nonpolarizable force fields. Note the strong propensity of the ions for the air/water interface.

the carboxylate groups wins over the hydrophobicity of the benzene ring and, consequently, the dianions prefer bulk aqueous solvation leaving an ion-free surface layer.

Although the results of the nonpolarizable and polarizable force fields are qualitatively similar upon closer inspection, there are subtle differences. Upon inclusion of polarization, which generally favors asymmetrically (i.e., interfacially) solvated structures,[26] the ion-free surface layer becomes thinner. Moreover, the isomers which have the two carboxylic groups located close to each other (i.e., the ortho- and, to a lesser extent, also the meta-isomers) tend to orient in the subsurface. This is seen in Figures 6a and 7a, where the signal from the carbon atoms of the benzene ring is shifted toward the surface compared to that of the carboxylate oxygens.

The hydration shell around the dicarboxylate dianions is not symmetric due to the different affinity of the $-COO^-$ groups vs the benzene ring for water. This is similar to the situation for dicarboxylate dianions with an aliphatic spacer group (such as adipate) investigated in our previous study.[9] As a demonstration, Figure 9 depicts the nearest 25 water molecules around the *p*-benzene dicarboxylate dianion from a typical snapshot from the simulation. While the water structure around the carboxylate groups is dense and compact, one clearly sees the diluted structure and voids in the solvent around the benzene ring.

A simple way to shift the balance between hydrophilic and hydrophobic interactions is via methylation. Figure 10 shows the density profiles for the tetramethyl-*o*-benzene dicarboxylate employing both polarizable and nonpolarizable force fields. The takeover of the hydrophobic interactions caused by (tetra)-methylation is obvious from the strong interfacial carbon and oxygen peaks. The heights and positions of these peaks are almost uninfluenced by the inclusion of polarization, confirming our previous finding that polarization effects are rather unimportant for strong (hydrophobic) ionic surfactants, such as tetrabutylammonium.[27] It also follows from Figure 10 that the sodium counterions, which inherently favor bulk solvation, are pulled toward the interface by attractive interactions to the dianions.

The tetramethyl-*o*-benzene dicarboxylate dianions are strongly oriented at the water/vacuum interface as demonstrated by a snapshot from the simulation (see Figure 11). Figure 12 shows the statistically average data, i.e., the distribution of orientations of the molecular axis of the dianion (passing through the center of the benzene ring between the two carboxylate groups) with respect to the normal to the surface. This nonuniform distribution sharply raises at small angles, peaking around 45° and having a long tail up to 150°. This indicates a preferential orientation with the two $-COO^-$ groups anchored in the interfacial water layer and with the benzene ring pointing into the gas phase but strongly tilted or lying on the surface.

Conclusions

Solvation of benzene dicarboxylate dianions in water clusters and in aqueous slabs was investigated by means of photoelectron spectroscopy and molecular dynamics simulations. Photoelectron spectra of the ortho- and para-isomers with up to 25 water molecules indicate interior solvation of the dianions. For the para-isomer an even−odd effect in the electron detachment

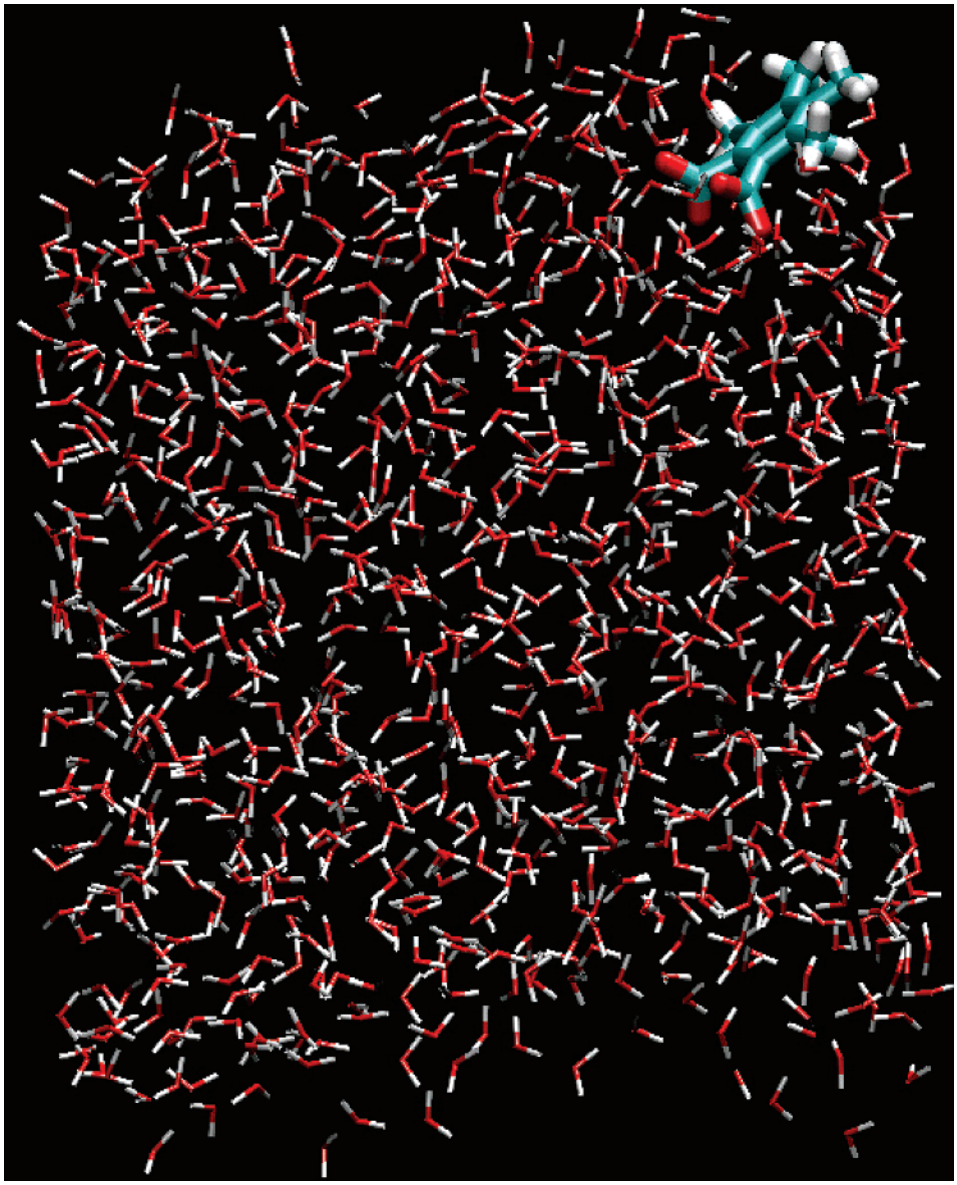

Figure 11. Snapshot from the molecular dynamics simulation depicting the tetramethyl-*o*-BCD^{2-} at the air/water interface. Note the preferential orientation of the dianion with the hydrophilic $-COO^-$ groups "anchored" in the aqueous phase and the hydrophobic methylated benzene ring tilted and pointing toward the gas phase.

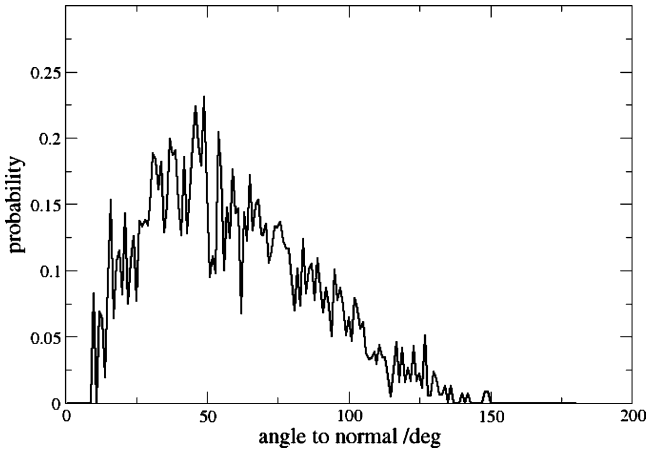

Figure 12. Orientation of the molecular axis of the tetramethyl-*o*-BCD^{2-}, passing through the center of the benzene ring between the two carboxylate groups, with respect to the normal to the surface (weighted by the factor $1/(\sin\theta)$). The peak around 45° indicates a preferential orientation of the ion at the surface, with a tilted aromatic ring and carboxylate groups pointing toward the aqueous bulk.

energies was observed as a result of alternate solvation of the two separated charged carboxylate groups. This effect is weaker than in dicarboxylate dianions with an aliphatic spacer, since the two carboxylic groups can to some extent interact with each other via the polarizable benzene ring. No even−odd effect was observed for the ortho-isomer because each water molecule can solvate both carboxylate groups simultaneously due to their proximity.

Molecular dynamics simulations in extended slabs predict bulk solvation for all three isomers of benzene dicarboxylate dianions, regardless the use of a polarizable or nonpolarizable force field, consistent with the observation in the solvated clusters. Upon tetramethylations, however, the dianions exhibit surfactant activity. The preferential position of tetramethyl-*o*-benzene dicarboxylate dianion is thus at the water/vapor interface with the charged carboxylic groups anchored in the aqueous phase and the hydrophobic benzene ring essentially lying on the topmost water layer.

Acknowledgment. Support from the Czech Ministry of Education via Grants ME644 and LC512 and from the U.S.

National Science Foundation (NSF; Grants CHE 041312 and 0209719) is gratefully acknowledged. Part of the work in Prague was supported via the Research Project Z40550506. The experimental work was supported by the U.S. Department of Energy (DOE), Office of Basic Energy Sciences, Chemical Science Division, and performed at the W. R. Wiley Environmental Molecular Sciences Laboratory, a national scientific user facility sponsored by DOE's Office of Biological and Environmental Research and located at Pacific Northwest National Laboratory, operated for DOE by Battelle.

References and Notes

(1) Kawamura, K.; Umemoto, N.; Mochida, M.; Bertram, T.; Howell, S.; Huebert, B. J. *J. Geophys. Res., [Atmos.]* **2003**, *108*.

(2) Kawamura, K.; Ng, L. L.; Kaplan, I. R. *Environ. Sci. Technol.* **1985**, *19*, 1082.

(3) Choi, M. Y.; Chan, C. K. *Environ. Sci. Technol.* **2002**, *36*, 2422.

(4) Brooks, S. D.; Garland, R. M.; Wise, M. E.; Prenni, A. J.; Cushing, M.; Hewitt, E.; Tolbert, M. A. *J. Geophys. Res., [Atmos.]* **2003**, *108*.

(5) Kerminen, V. M. *J. Geophys. Res., [Atmos.]* **2001**, *106*, 17321.

(6) Kerminen, V. M.; Ojanen, C.; Pakkanen, T.; Hillamo, R.; Aurela, M.; Merilainen, J. *J. Aerosol Sci.* **2000**, *31*, 349.

(7) Seinfeld, J. H.; Pankow, J. F. *Annu. Rev. Phys. Chem.* **2003**, *54*, 121.

(8) Yang, X.; Fu, Y. J.; Wang, X. B.; Slavicek, P.; Mucha, M.; Jungwirth, P.; Wang, L. S. *J. Am. Chem. Soc.* **2004**, *126*, 876.

(9) Minofar, B.; Mucha, M.; Jungwirth, P.; Yang, X.; Fu, Y. J.; Wang, X. B.; Wang, L. S. *J. Am. Chem. Soc.* **2004**, *126*, 11691.

(10) Fujii, M.; Shinohara, N.; Lim, A.; Otake, T.; Kumagai, K.; Yanagisawa, Y. *Atmos. Environ.* **2003**, *37*, 5495.

(11) Wilkinson, C. F.; Lamb, J. C. *Regulatory Toxicol. Pharmacol.* **1999**, *30*, 140.

(12) Wang, L. S.; Ding, C. F.; Wang, X. B.; Barlow, S. E. *Rev. Sci. Instrum.* **1999**, *70*, 1957.

(13) Wilson, M. A.; Pohorille, A. *J. Chem. Phys.* **1991**, *95*, 6005.

(14) Essmann, U.; Perera, L.; Berkowitz, M. L.; Darden, T.; Lee, H.; Pedersen, L. G. *J. Chem. Phys.* **1995**, *103*, 8577.

(15) Ryckaert, J.-P.; Ciccotti, G.; Berendsen, H. J. C. *J. Comput. Phys.* **1977**, *23*, 327.

(16) Berendsen, H. J. C.; Grigera, J. R.; Straatsma, T. P. *J. Phys. Chem.* **1987**, *91*, 6269.

(17) Caldwell, J. W.; Kollman, P. A. *J. Phys. Chem.* **1995**, *99*, 6208.

(18) Wang, J. M.; Wolf, R. M.; Caldwell, J. M.; Kollman, P. A.; Case, D. A. *J. Comput. Chem.* **2004**, *25*, 1157.

(19) Case, D. A. D., T. A.; Cheatham, T. E., III.; Simmerling, C. L.; Wang, J.; Duke, R. E.; Luo, R.; Merz, K. M.; Wang, B.; Pearlman, D. A.; Crowley, M.; Brozell, S.; Tsui, V.; Gohlke, H.; Mongan, J.; Hornak, V.; Cui, G.; Beroza, P.; Schafmeister, C.; Caldwell, J. W.; Ross, W. S.; Kollman, P. A. *Amber 8*; University of California: San Francisco, 2004.

(20) Frisch, M. J.; Trucks, G. W.; Schlegel, H. B.; Scuseria, G. E.; Robb, M. A.; Cheeseman, J. R.; Zakrzewski, V. G.; Montgomery, J. A., Jr.; Stratmann, R. E.; Burant, J. C.; Dapprich, S.; Millam, J. M.; Daniels, A. D.; Kudin, K. N.; Strain, M. C.; Farkas, O.; Tomasi, J.; Barone, V.; Cossi, M.; Cammi, R.; Mennucci, B.; Pomelli, C.; Adamo, C.; Clifford, S.; Ochterski, J.; Petersson, G. A.; Ayala, P. Y.; Cui, Q.; Morokuma, K.; Malick, D. K.; Rabuck, A. D.; Raghavachari, K.; Foresman, J. B.; Cioslowski, J.; Ortiz, J. V.; Stefanov, B. B.; Liu, G.; Liashenko, A.; Piskorz, P.; Komaromi, I.; Gomperts, R.; Martin, R. L.; Fox, D. J.; Keith, T.; Al-Laham, M. A.; Peng, C. Y.; Nanayakkara, A.; Gonzalez, C.; Challacombe, M.; Gill, P. M. W.; Johnson, B. G.; Chen, W.; Wong, M. W.; Andres, J. L.; Head-Gordon, M.; Replogle, E. S.; Pople, J. A. *Gaussian 98*; Gaussian, Inc.: Pittsburgh, PA, 1998.

(21) Wang, X. B.; Nicholas, J. B.; Wang, L. S. *J. Chem. Phys.* **2000**, *113*, 653.

(22) Wang, L. S., Ding, C. F., Wang, X. B., Nicholas, J. B. *Phys. Rev. Lett.* **1998**, *81*, 2667.

(23) Wang, X. B.; Yang, X.; Nicholas, J. B.; Wang, L. S. *Science* **2001**, *294*, 1322.

(24) Yang, X.; Wang, X. B.; Wang, L. S. *J. Phys. Chem. A* **2002**, *106*, 7607.

(25) Wang, X. B.; Yang, X.; Nicholas, J. B.; Wang, L. S. *J. Chem. Phys.* **2003**, *119*, 3631.

(26) Vrbka, L.; Mucha, M.; Minofar, B.; Jungwirth, P.; Brown, E. C.; Tobias, D. J. *Curr. Opin. Colloid Interface Sci.* **2004**, *9*, 67.

(27) Winter, B.; Weber, R.; Schmidt, P. M.; Hertel, I. V.; Faubel, M.; Vrbka, L.; Jungwirth, P. *J. Phys. Chem. B* **2004**, *108*, 14558.